Modified Koch Fractal Antenna for Multi and Wideband Wireless Applications

Shweta Rani[1†] and **Sushil Kakkar**[2], Non-members

ABSTRACT

This paper focuses on the design and development of modified Koch fractal antenna. Compared to traditional Koch curve antenna, the presented antenna possesses a greater number of frequency bands and better impedance matching. Furthermore, the bacterial foraging optimization (BFO) approach is implemented to enhance the impedance bandwidth. The developed technique has been verified by employing various numerical simulations. The design parameters generated from the optimization procedure have been utilized to manufacture the antenna and the respective experimental and simulated results compared. The measured results show that the designed antenna exhibits multi and wideband behavior, covering WLAN, WIMAX, and various other wireless applications.

Keywords: Bacterial Foraging Optimization, BFO, Bandwidth, Fractal Antenna

1. INTRODUCTION

Various technologies are often integrated to develop multifunctional microstrip patch antennas. Such a task becomes much harder each time a high degree of miniaturization is required [1]. Due to their space filling properties, fractal geometries have always been considered to be a better option for miniaturized multiband antennas [2]. However, it is a complicated task to design the fractal antenna geometry according to user-defined applications [3–5]. Recently, antenna system engineers have attempted to critically explore the dimensional behavior of fractal geometries. Therefore, geometries irregular in nature are becoming popular because of their capability to provide wider bandwidth and multiband operation [6]. Rani *et al.* (2013) [7] depicted that by modifying the Koch fractal geometry, the multiband behavior of such antennas can be regulated. In addition, these modifications equip the design engineer with a tool to make the structures useful for wideband applications. Ali *et al.* (2012) [8] implemented Koch's second iteration fractal geometry to shape the antenna ground plane for augmenting the wideband property. Taking a similar approach, Gorai *et al.* (2013) [9] used Koch's fractal curve to etch a slot on the UWB antenna responsible for creating the notched band. However, such efforts do not rely on any standard mathematical formula and the corresponding results very much depend on the antenna under observation. Therefore, repetitive simulation is required to obtain the final fractal antenna design [10, 11].

Nowadays, soft computing techniques have become ubiquitous among researchers, academicians, and analysts in pretty much every part of design engineering. An alternative method, namely bacterial foraging optimization (BFO) is gaining in popularity for optimizing parameters in antenna and antenna array problems [12]. The basics of BFO depend on the point at which animals with poor foraging techniques are eradicated, while those with successful foraging techniques survive and grow. Animals with weak foraging techniques are either eradicated or reformed into better ones [13]. The E. coli bacterium present in human intestines have a foraging strategy consisting of four processes: chemotaxis, swarming, reproduction, and elimination and dispersal [14–16]. Mandal *et al.* (2011) [17] adopted BFO to optimize the design, current excitation weights, and radii of a three-ring concentric circular antenna array to obtain the maximum reduction in the sidelobe level (SLL).

This paper demonstrates the design and development of modified Koch fractal antenna using the BFO algorithm for various multi and wideband wireless applications. In this paper, the BFO technique is implemented to optimize the dimensional parameters of the antenna.

2. ANTENNS DESIGN AND STRUCTURE

The self-similar behavior of fractal shapes enables them to replicate throughout the structure. Modifications in fractal geometries provide an extra degree of freedom in antenna design and open up

Manuscript received on September 27, 2020 ; revised on December 25, 2020 ; accepted on February 23, 2021. This paper was recommended by Associate Editor Susamay Samanta.

[1]The author is with the Department of Electronics & Communication Engineering, Giani Zail Singh Campus College of Engineering and Technology, Maharaja Ranjit Singh Punjab Technical University, Bathinda, Punjab, India.

[2]The author is with the Department of Electronics & Communication Engineering, Bhai Gurdas Institute of Engineering and Technology, Punjab, India.

†Corresponding author: shwetaranee@gmail.com

Digital Object Identifier 10.37936/ecti-eec.2021192.242065

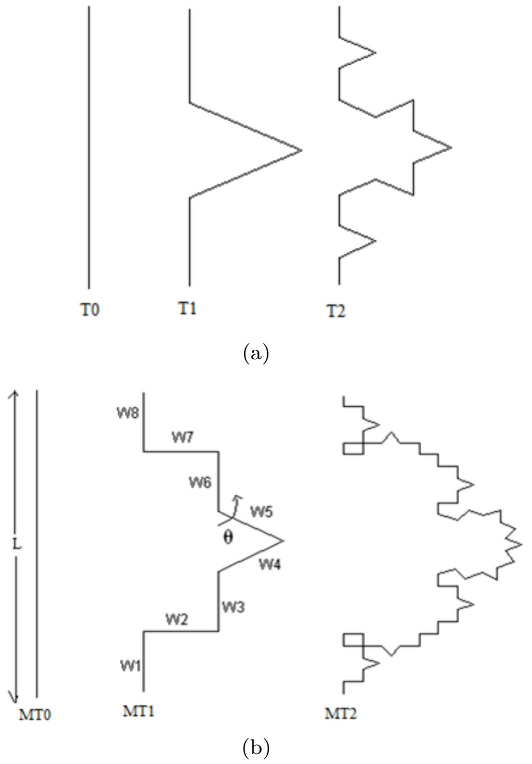

Fig. 1: *Geometry of (a) traditional Koch curve and (b) proposed modified Koch curve.*

a wide range of application possibilities. Similarly, the proposed modified Koch fractal antenna with different iteration orders is designed using a scale factor of 1/5, without varying the actual physical parameters of the microstrip patch. The presented structure of fractal is built utilizing the iterated function system (IFS) to obtain successive iterations. Fig. 1 shows the geometry of the traditional Koch curve and proposed modified Koch curve with the three iterations being zero (MT0), first (MT1), and second (MT2), where L is the length of the element and θ is the indentation angle. Since higher order iterations of the presented geometry do not produce any significant contribution in terms of resonant performance, only the first and second iterations are taken into account here. The antenna is designed on an easily available and cost-effect FR4 substrate where thickness $h = 1.6$ mm with a dielectric constant of $\varepsilon_r = 4.4$. The ground dimensions of the printed geometry are characterized by the ground plane length where $Y = 30$ mm and the ground plane width where $X = 30$ mm.

2.1 IFS Algorithm for the Modified Koch Curve

The IFS technique provides the vertices for the next iteration of fractal geometry. In the existing literature, so far, the number of fractal geometries has been developed using the iterated function system. The mathematics involved in the technique consist of several complex transformations [4]. The following equations are required to obtain the segments of the generator (MT1):

$$W1\begin{pmatrix} x' \\ y' \end{pmatrix} = \begin{bmatrix} 1/5 & 0 \\ 0 & 1/5 \end{bmatrix}\begin{pmatrix} x \\ y \end{pmatrix} \tag{1}$$

$$W2\begin{pmatrix} x' \\ y' \end{pmatrix} = \begin{bmatrix} 0 & 1/5 \\ -1/5 & 0 \end{bmatrix}\begin{pmatrix} x \\ y \end{pmatrix} + \begin{pmatrix} 0 \\ 1/5 \end{pmatrix} \tag{2}$$

$$W3\begin{pmatrix} x' \\ y' \end{pmatrix} = \begin{bmatrix} 1/5 & 0 \\ 0 & 1/5 \end{bmatrix}\begin{pmatrix} x \\ y \end{pmatrix} + \begin{pmatrix} 1/5 \\ 1/5 \end{pmatrix} \tag{3}$$

$$W4\begin{pmatrix} x' \\ y' \end{pmatrix} = \begin{bmatrix} 1/10 & \sqrt{3}/10 \\ -\sqrt{3}/10 & 1/10 \end{bmatrix}\begin{pmatrix} x \\ y \end{pmatrix} + \begin{pmatrix} 1/5 \\ 2/5 \end{pmatrix} \tag{4}$$

$$W5\begin{pmatrix} x' \\ y' \end{pmatrix} = \begin{bmatrix} 1/10 & -\sqrt{3}/10 \\ \sqrt{3}/10 & 1/10 \end{bmatrix}\begin{pmatrix} x \\ y \end{pmatrix} + \begin{pmatrix} 0.3732 \\ 0.5 \end{pmatrix} \tag{5}$$

$$W6\begin{pmatrix} x' \\ y' \end{pmatrix} = \begin{bmatrix} 1/5 & 0 \\ 0 & 1/5 \end{bmatrix}\begin{pmatrix} x \\ y \end{pmatrix} + \begin{pmatrix} 1/5 \\ 3/5 \end{pmatrix} \tag{6}$$

$$W7\begin{pmatrix} x' \\ y' \end{pmatrix} = \begin{bmatrix} 0 & -1/5 \\ 1/5 & 0 \end{bmatrix}\begin{pmatrix} x \\ y \end{pmatrix} + \begin{pmatrix} 1/5 \\ 4/5 \end{pmatrix} \tag{7}$$

$$W8\begin{pmatrix} x' \\ y' \end{pmatrix} = \begin{bmatrix} -1/5 & 0 \\ 0 & 1/5 \end{bmatrix}\begin{pmatrix} x \\ y \end{pmatrix} + \begin{pmatrix} 0 \\ 4/5 \end{pmatrix} \tag{8}$$

The above transformation has been used to obtain the generator for the proposed geometry, given as the following equation:

$$\begin{aligned} T1 = {} & W1(T) \cup W2(T) \cup W3(T) \cup W4(T) \\ & \cup W5(T) \cup W6(T) \cup W7(T) \cup W8(T) \end{aligned} \tag{9}$$

The fractal or similarity dimension is an essential property of the fractal structure, since it is used to determine a group of geometries with common behavior. Hence, the fractal dimension is always considered first when utilizing fractal geometry in antenna design. The similarity dimension of the proposed fractal geometry may be derived using the following equation where R is the scale factor and M is the number of distinct scaled copies [5]:

$$D = \frac{\log M}{\log 1/R} = \frac{\log 8}{\log 5} = 1.293 \tag{10}$$

2.2 BFO Implementation

In the BFO method, a bunch of bacteria proceed to look for food far away from poisonous elements. All bacteria attempt to move independently upward toward the maximum food density. At the starting position, they measure the food density. They then tumble in an arbitrary direction, swim for a fixed distance, and measure the food density. This tumble and swim process constitutes one chemotactic step.

Table 1: *Input parameters of the BFO.*

Parameters	Details	Values
T	Population of bacteria	10
C_n	Chemotactic step count	20
S_n	Length of swim	4
R_n	Count of reproduction steps	4
ED_n	Count of elimination-dispersal events	2
P_{ED}	Probability of elimination-dispersal step	0.25

When there is more food density at the next location, they take another stride toward it. If the food is less dense at the next location compared to the previous one, they tumble again to look for another direction, and swim toward it. This process continues for a definite number of steps, further restricted by the life of the bacterium. Toward the end of their lifetimes, the healthy bacteria in a substantially dense region split into two cells. The successive generation in the next reproductive step therefore starts from a healthy position. The healthy portion of bacteria reproduces the next generation, whereas the unhealthy bacteria die. This reproduction step is likewise completed a fixed number of times [13–15].

In this study, the BFO performs the crucial role of acquiring the optimized value for the dimensional parameter, with an indentation angle of θ. This denotes the best possible geometry for the required multiband and wideband functions. The most relevant higher and lower bounds are employed to generate a single dimensional solution space in which BFO seeks the best parametric value for the proposed geometry. At that point, a fitness is obtained, giving a solitary number, subsequent to taking the values of this parameter. The input parameters for the BFO are presented in Table 1, tuned to solve the fitness function for multi and wideband operation.

3. RESULTS AND DISCUSSION

3.1 Resonant Performance of the Modified Koch Fractal Antenna

In this study, the IE3D EM simulator is adopted to assess the performance of the presented antennas. This simulator is based on the method of moments and utilizes it extensively to evaluate the complex integral electric field equations. The S_{11} parameters of all the three iterations presented in this work are depicted in Fig. 2. As can be observed, the resonant frequency of the antennas shifts toward the left side with every iteration increment. These results satisfy the fractals' space filling properties due to an increase in the electrical length of the antenna. The results illustrate that the proposed antenna geometry also fulfills the self-similarity property of the fractal structure while possessing multifrequency operational characteristics.

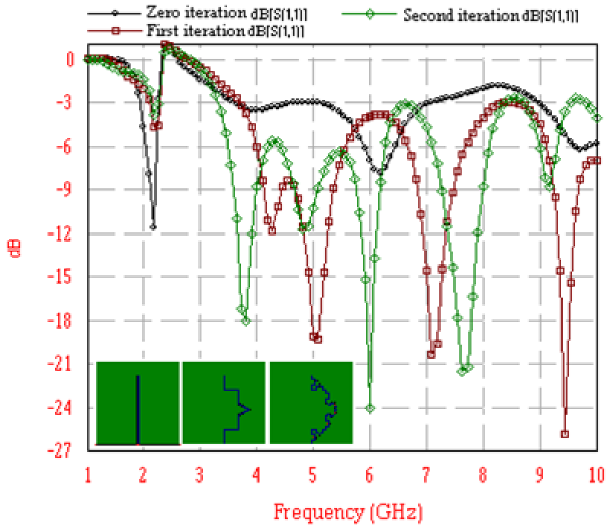

Fig. 2: *S_{11} parameter of the modified Koch fractal antenna for all three iterations.*

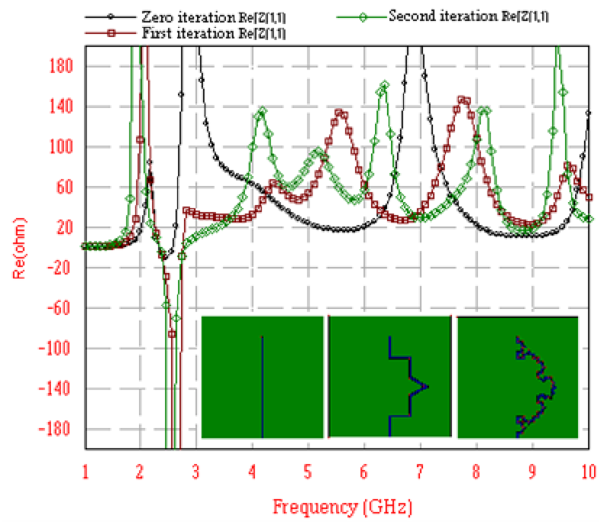

Fig. 3: *Real input impedance of the modified Koch fractal antenna for all three iterations.*

A resistance connected in series with a reactance constitutes the antenna's terminal impedance for a frequency at resonance. This can be represented by the following equation.

$$Z_T = R_T + j\left(\omega L_T - \frac{1}{\omega C_T}\right) \tag{11}$$

where ω is the resonant frequency. Z_T, R_T, L_T, and C_T are the impedance, resistance, inductance, and capacitance of the proposed antenna, respectively. To efficiently match the antenna impedance to the feed line, the adoption of an effective design procedure provides minimum back reflection to the source. A graphical plot of the input impedance for all three iterations of the proposed modified Koch fractal antenna is shown in Fig. 3. Interestingly, both

Table 2: *Comparative analysis of the 1st iteration.*

Traditional Koch curve antenna			
Resonant frequency (GHz)	Reflection coefficient (dB)	Input impedance (Ω)	Bandwidth (percentage)
5.36	−18.90	47.51	4.47
7.72	−20.68	49.83	5.86
Modified Koch curve antenna			
Resonant frequency (GHz)	Reflection coefficient (dB)	Input impedance (Ω)	Bandwidth (percentage)
4.27	−11.90	57.14	4.26
5.09	−19.36	61.44	7.02
7.09	−20.39	41.61	5.98
9.45	−25.85	50.48	2.80

Table 3: *Comparative analysis of the 2nd iteration.*

Traditional Koch curve antenna			
Resonant frequency (GHz)	Reflection coefficient (dB)	Input impedance (Ω)	Bandwidth (percentage)
5.27	−11.49	40.86	7.47
7.45	−10.75	33.45	2.41
9.36	−14.14	36.23	3.85
Modified Koch curve antenna			
Resonant frequency (GHz)	Reflection coefficient (dB)	Input impedance (Ω)	Bandwidth (percentage)
3.81	−18.10	49.99	7.24
4.90	−11.62	74.46	7.01
6.00	−24.12	55.73	5.97
7.63	−21.54	52.30	7.14

the input and bandwidth impedances experience a considerable improvement with each subsequent iteration of the fractal geometry.

3.2 Comparison between the Traditional Koch Fractal Antenna and Its Modified Structure

This section presents a comparison between the modified Koch fractal antenna and its traditional counterpart with height L from end to end being constant for both structures. Modifications to the traditional geometry show an unprecedented improvement in the resonating properties of antenna. As can be observed from the available data in Tables 2 and 3, the modified Koch fractal antenna exhibits multifrequency operation and outperforms its traditional counterpart in terms of reflection coefficient, input impedance, and bandwidth for both the considered iterations.

Table 4: *Comparison of proposed antenna with and without optimization.*

Modified Koch curve antenna (without optimization)			
Resonant frequency (GHz)	Reflection coefficient (dB)	Input impedance (Ω)	Bandwidth (percentage)
3.81	−18.10	49.99	7.24
4.90	−11.62	74.46	7.01
6.00	−24.12	55.73	5.97
7.63	−21.54	52.30	7.14
Modified Koch curve antenna (with optimization)			
Resonant frequency (GHz)	Reflection coefficient (dB)	Input impedance (Ω)	Bandwidth (percentage)
3.63	−14.57	51.29	4.90
5.81	−23.72	49.46	13.04
7.54	−16.77	48.89	30.10
9.54	−21.54	55.16	23.71

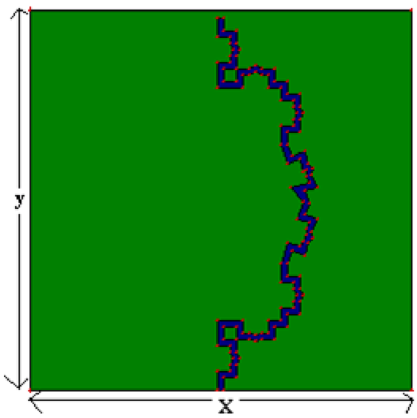

Fig. 4: *Geometry of the optimized antenna.*

3.3 Optimization Results

The design method used in this study can potentially give rise to an optimization issue and this is resolved by employing the BFO. The advantage of the BFO is its ability to discover the optimized design parameter (θ) of the modified Koch fractal antenna. The performance effectiveness of the antenna is determined by its electrical size, which is controlled by the indentation angle (θ). Fig. 4 shows the proposed geometry of the optimized structure, where X and Y are ground plane dimensions, each equal to 30 mm. The optimized indentation angle for the modified Koch fractal antenna is 18°. The comparative results of the modified Koch curve fractal antenna with and without implementation of the optimization technique are reported in Table 4. The results illustrate that the proposed antenna with optimization has better resonating properties than its common model (without optimization) in

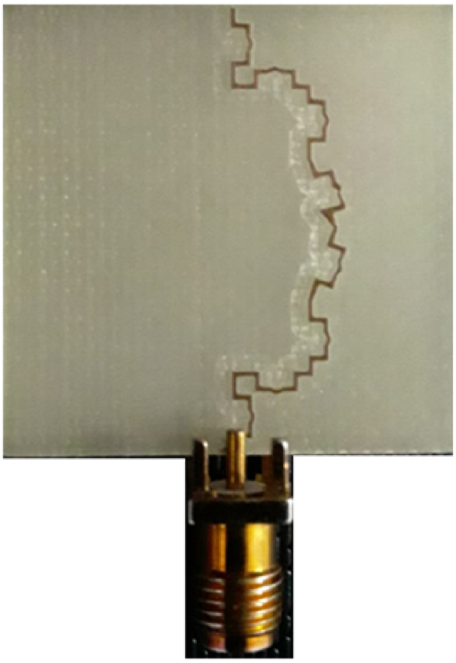

Fig. 5: *Photograph of the fabricated prototype.*

a factually significant way. The optimized antenna has a maximum achievable bandwidth of 30.10% in comparison to the 7.24% exhibited by the common model of the proposed antenna at frequency bands of 7.54 GHz and 3.81 GHz, respectively. In addition, the optimized antenna also provides a better reflection coefficient and input impedance than the antenna without optimization.

3.4 Experimental Results

The presented antenna geometry has been optimized with the goal of increasing the wide and multiband properties of the antenna. The model has been fabricated utilizing standard printed circuit strategy according to the configuration determined by employing the BFO procedure; such that the indentation angle (θ) is 18°. A photograph of the fabricated antenna model is shown in Fig. 5. A comparison plot of the measured and simulated results is shown in Fig. 6. It can be observed from the presented results that the proposed structure exhibits multi and wideband behavior, resonating at 3.36 GHz (3.20–3.52 GHz), 5.61 GHz (4.75–5.80 GHz), 7.27 GHz and 9.27 GHz (6.95–9.54 GHz) covering WLAN, WIMAX, and various other wireless applications. Furthermore, after optimization, bandwidth enhancements of about 3%, 13.1%, and 24.26% for the first, second, and third frequency bands, respectively, is revealed by both measurement and simulated results. Except for a slight frequency movement, the measurement shows good agreement with the simulated results. This frequency movement is generally due to imperfections occurring during fabrication.

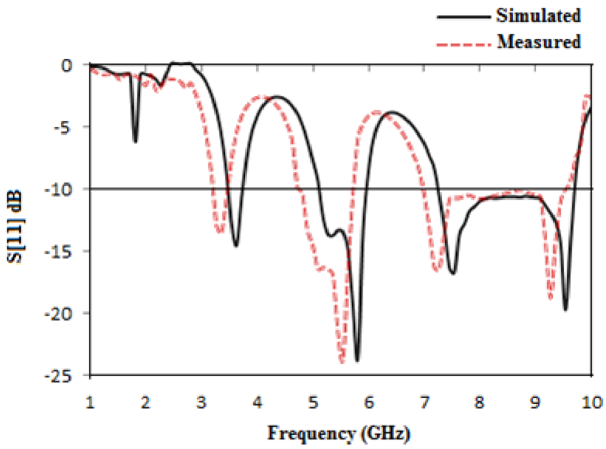

Fig. 6: *Comparison plot between the simulated and measured S_{11} parameters of the modified Koch fractal antenna.*

3.5 Radiation Patterns

The radiation characteristics of the modified Koch fractal antenna were measured in the frequency domain of an anechoic chamber. The fabricated prototype was placed in the receiver position with a standard horn antenna utilized as the transmitter. Fig. 7 presents the simulated and measured radiation patterns of all resonating frequencies. The results indicate that the proposed antenna provides good omnidirectional radiation pattern in the H-plane and dipole-like radiation patterns in the E-plane. In addition, the presented antenna is found to be linearly co-polarized and provides feasible radiation performance at all frequency bands.

3.6 Gains Exhibited by Modified Koch Fractal Antenna

A comparative graph of the simulated and measured gains of the proposed antenna is shown in Fig. 8. The maximum measured gain of the modified Koch fractal antenna is 4.89 dBi at a resonant frequency of 9.27 GHz. The difference between the full-wave measurements and simulation might be due to the standard connectors, dispersive nature of the FR4 dielectric material, and manufacturing tolerances.

3.7 Comparison

A comparative study of the proposed antenna and other models in the existing literature is presented in Table 5. The details reveal that the proposed antenna outperformed in terms of bandwidth and other antenna characteristics. Furthermore, the size of the proposed antenna is significantly smaller because of its fractal geometry.

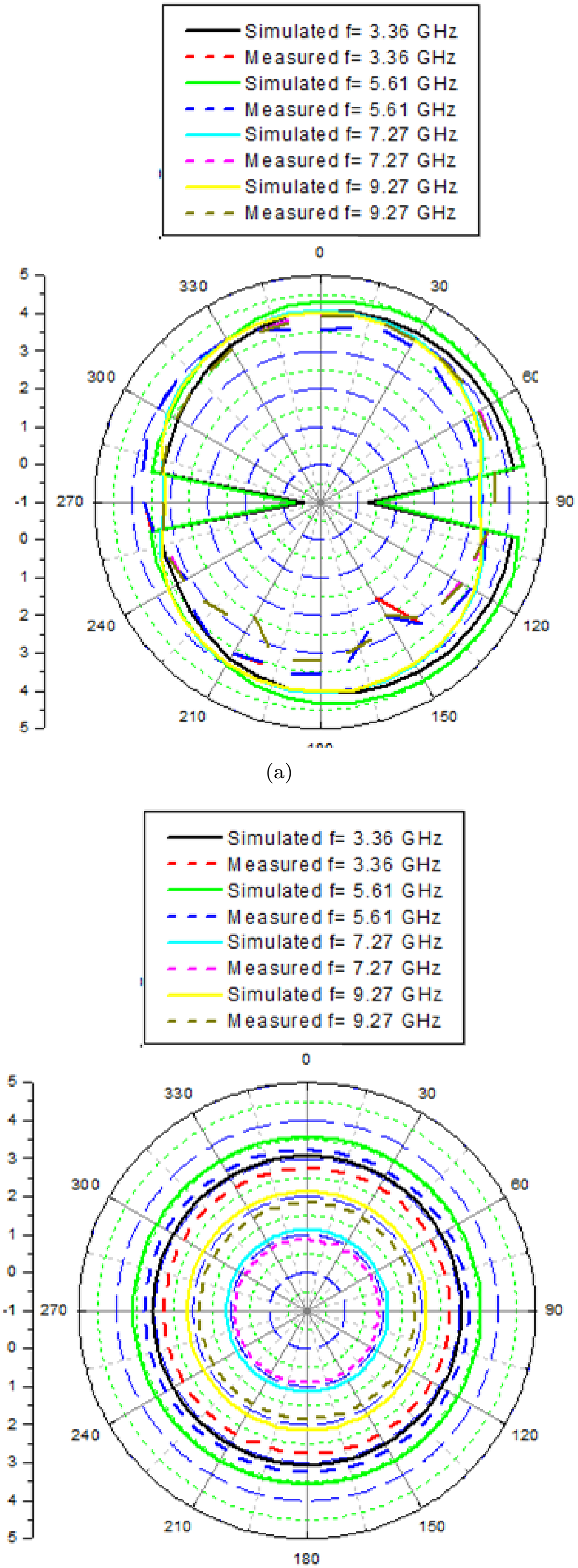

Fig. 7: *Simulated and measured radiation patterns of the proposed modified Koch fractal antenna; (a) E-plane and (b) H-plane.*

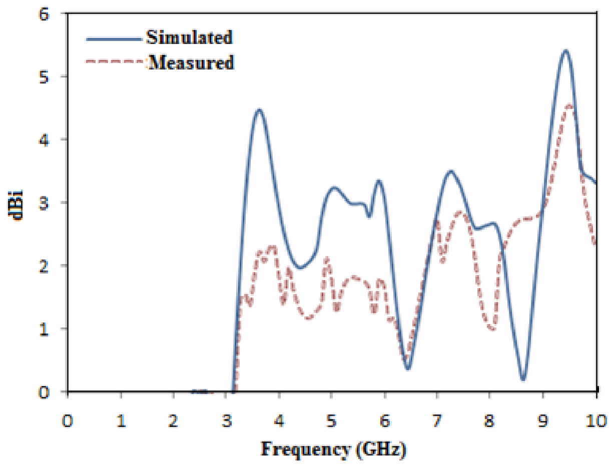

Fig. 8: *Gains exhibited by the modified Koch fractal antenna.*

Table 5: *Comparative study of the proposed antenna and previously published works.*

Ref.	Description	Size (mm)	Resonating Frequency (GHz)	Bandwidth (%)	Gain (dBi)
[18]	Fractal multiband antennas based on lotus-pod patterns	Radius = 65.2	0.636	2.9	3.0
			1.136	2.5	–
			1.6	4.0	–
			1.88	2.5	–
			2.11	4.3	–
			2.5	5.0	–
			2.95	4.2	–
[19]	Antenna with circular DGS	40 × 28	2.45	6.5	4.72
			3.5	4.18	6.2
			5.28	4.97	3.8
[20]	Monopole antenna using DGS	30 × 20	2.31	16	2.46
			3.42	27	2.45
			5.44	16	3.0
Proposed	Modified Koch fractal antenna	30 × 30	3.36	9.3	1.71
			5.61	20.03	1.89
			7.27	31.81	2.35
			9.27	27.93	4.89

4. CONCLUSION

The aim of this paper was to explore a modified design of the Koch fractal antenna which can outperform earlier versions to provide multi and wideband responses. The BFO approach was utilized in this study to determine the geometrical descriptor for the proposed fractal antenna. The antenna prototype was effectively employed to validate the feasibility of the developed structure. The proposed antenna was found to radiate omnidirectional patterns at all operating frequency bands, making it suitable for WLAN, WiMAX, and various other wireless applications.

REFERENCES

[1] D. Li and J. Mao, "A Koch-like Sided Fractal Bow-Tie Dipole Antenna," *IEEE Transactions on Antennas and Propagation*, vol. 60, no. 5, pp. 2242–2251, 2012.

[2] D. H. Werner and S. Ganguly, "An Overview of Fractal Antenna Engineering Research," *IEEE Antennas and Propagation Magazine*, vol. 45, no. 1, pp. 38–57, 2003.

[3] L. Lizzi, R. Azaro, G. Oliveri, and A. Massa, "Printed UWB Antenna Operating Over Multiple Mobile Wireless Standards," *IEEE Antennas and Wireless Propagation Letters*, vol. 10, pp. 1429–1432, 2011.

[4] K. J. Vinoy, J. K. Abraham, and V. K. Varadan, "On the Relationship between Fractal Dimension and the Performance of Multi-Resonant Dipole Antennas Using Koch Curves," *IEEE Transactions on Antennas and Propagation*, vol. 51, no. 9, pp. 2296–2303, 2003.

[5] M. Comisso, "Theoretical and Numerical Analysis Of The Resonant Behaviour of The Minkowski Fractal Dipole Antenna," *IET Microwaves, Antennas & Propagation*, vol. 3, no. 3, pp. 456–464, 2009.

[6] S. Rani and A. P. Singh, "On the Design and Optimization Of New Fractal Antenna Using PSO," *International Journal of Electronics*, vol. 100, no. 10, pp. 1383–1397, 2012.

[7] S. Rani and A. P. Singh, "Modified Koch Fractal Antenna With Asymmetrical Ground Plane For Multi And UWB Applications," *International Journal of Applied Electromagnetics and Mechanics*, vol. 42, no. 2, pp. 259–267, 2013.

[8] J. K. Ali, A. J. Salim, A. I. Hammoodi, and H. Alsaedi, "An Ultra-Wide Band Printed Monopole Antenna With Fractal Based Reduced Ground Plane," in *Progress in Electromagnetics Research Symposium Proceedings*, Moscow, Russia, 2012, pp. 613–617.

[9] A. Gorai, A. Karmakar, M. Pal, and R. Ghatak, "Multiple Fractals –Shaped Slots Based UWB Antenna With Triple-Band Notch Functionality," *Journal of Electromagnetic Waves and Applications*, vol. 27, no. 18, pp. 2407–2415, 2013.

[10] S. Kakkar and S. Rani, "Implementation of Fractal Geometry to Enhance The Bandwidth of CPW Fed Printed Monopole Antenna," *IETE Journal of Research*, vol. 63, no. 1, pp. 23–30, 2017.

[11] M. Jahromi, A. Falahati, and R. Edwards, "Bandwidth and Impedance Matching Enhancement of Fractal Monopole Antennas Using Compact Grounded Co-Planar Waveguide," *IEEE Transactions on Antennas and Propagation*, vol. 59, no. 7, pp. 48–56, 2011.

[12] K. Passino, "Biomimicry of Bacterial Foraging For Distributed Optimization And Control," *IEEE Control Systems Magazine*, vol. 22, no. 3, pp. 52–67, 2002.

[13] T. Datta and I. Misra, "A Comparative Study of Optimization Techniques in Adaptive Antenna Array Processing: The Bacteria-Foraging Algorithm and Particle Swarm Optimization," *IEEE Antennas and Propagation Magazine*, vol. 51, no. 6, pp. 69–81, 2009.

[14] M. Tripathy and S. Mishra, "Bacteria Foraging-Based Solution to Optimize Both Real Power Loss And Voltage Stability Limit," *IEEE Transactions on Power Systems*, vol. 22, no. 1, pp. 240–248, 2007.

[15] B. Mangaraj, I. Misra, and A. Barisal, "Optimizing Included Angle of Symmetrical V-Dipoles For Higher Directivity Using Bacteria Foraging Optimization Algorithm" *Progress in Electromagnetic Research B*, vol. 3, pp. 295–314, 2008.

[16] S. Sharma and B. Kanujia, "Optimization of Resonant Frequency of Circular Microstrip Antenna With And Without Air Gaps Using Bacterial Foraging Optimization Technique," in *IEEE International Conference on Computational Intelligence and Communication Systems*, 2011, pp. 574–577.

[17] D. Mandal, R. Kar, and S. P. Ghosal, "Bacterial Foraging Optimization Based Synthesis of Concentric Circular Antenna Array," in *IEEE International Conference on Recent Trends in Information Systems*, Kolkata, India, 2011, pp. 99–104.

[18] J. Liu , Y. Liu, D. Chang, C. Chang, and C. Cheng, "Fractal Multiband Antennas based on Lotus Pod Patterns," *Microwave and Optical Technology Letters*, vol. 30, no. 3, pp. 223–228, 2002.

[19] B. R. S. Reddy and D. Vakula, "Compact Zigzag-Shaped-Slit microstrip antenna with circular defected ground structure for wireless applications," *IEEE Antenna and Wireless Propagation Letters*, vol. 14, pp. 678–681, 2015.

[20] W. Liu, C. Wu, and Y. Dai, "Design of triple frequency microstrip fed monopole antenna using defected ground structure," *IEEE Transactions on Antennas and Propagation*, vol. 59, no. 7, pp. 2457–2463, 2011.

Shweta Rani received her B.Tech degree from Punjab Technical University, India in 2003 and M.E. degree from Thapar University, Patiala, India in 2006. She received her Ph.D. degree in 2014 in the field of fractal antennas from the Department of Electronics and Communication Engineering, Sant Longowal Institute of Engineering & Technology, Punjab, India. At present, she is an assistant professor in the

Department of Electronics and Communication Engineering at Giani Zail Singh Campus College of Engineering and Technology, Bathinda, Punjab, India. She has 10 years of teaching experience. She received "Young Engineers Award" in October 2015 from Institution of Engineers (India). She has published more than 60 research papers in various international and national journals/conferences. She has received various awards and recognitions including KF Antia Award by the Institution of Engineers (India) in 2014 and best paper awards in four different international and national conferences. Besides convener of 2 international conferences ICAET 2015 and 2016, she has been the active organizing member of various faculty development programs, workshops, and conferences.

Sushil Kakkar received his B.Tech, M.Tech and Ph.D. degrees from I. K. Gujral Punjab Technical University (PTU), Jalandhar, Punjab, India. He has in his credit five best paper awards in five different international and national conferences. He has published more than 50 research papers in various national & international journals/conferences. Besides convener of 5 international conferences, he has been the active organizing member of various faculty development programs, workshops, webinars and conferences. His biography has been published in 32nd Edition of Who's Who in the World, 2015 by MARQUIS, New York. His research interests include microstrip antennas and biologically inspired computational techniques.